Journal of Hazardous Materials 189 (2011) 377–383

Contents lists available at ScienceDirect

Journal of Hazardous Materials

journal homepage: www.elsevier.com/locate/jhazmat

Biotemplated preparation of CdS nanoparticles/bacterial cellulose hybrid nanofibers for photocatalysis application

Jiazhi Yang[a], Junwei Yu[a], Jun Fan[b], Dongping Sun[a,*], Weihua Tang[a,**], Xuejie Yang[a]

[a] Key Laboratory of Soft Chemistry and Functional Materials (Ministry of Education), Nanjing University of Science and Technology, Nanjing 210094, People's Republic of China
[b] School of Environment, Nanjing University, Nanjing 210093, People's Republic of China

ARTICLE INFO

Article history:
Received 23 July 2010
Received in revised form 15 February 2011
Accepted 16 February 2011
Available online 23 February 2011

Keywords:
Bacterial cellulose
CdS nanoparticle
Nanofiber
Photocatalyst

ABSTRACT

In this work, we describe a novel facile and effective strategy to prepare micrometer-long hybrid nanofibers by deposition of CdS nanoparticles onto the substrate of hydrated bacterial cellulose nanofibers (BCF). Hexagonal phase CdS nanocrystals were achieved via a simple hydrothermal reaction between $CdCl_2$ and thiourea at relatively low temperature. The prepared pristine BCF and the CdS/BCF hybrid nanofibers were characterized by transmission electron microscopy (TEM), X-ray diffraction (XRD), thermogravimetric analysis (TGA), UV–vis absorption spectroscopy (UV–vis), and X-ray photoelectron spectroscopy (XPS). The results reveal that the CdS nanoparticles were homogeneously deposited on the BCF surface and stabilized via coordination effect. The CdS/BCF hybrid nanofibers demonstrated high-efficiency photocatalysis with 82% methyl orange (MO) degradation after 90 min irradiation and good recyclability. The results indicate that the CdS/BCF hybrid nanofibers are promising candidate as robust visible light responsive photocatalysts.

1. Introduction

Environmental pollution and destruction on a global scale have attracted much attention to the necessity of new, safe and clean chemical technologies and processes [1]. Photocatalysis is an efficient, attractive, and clean technology for pollutant abatement either in aqueous media or in the gas phase [2]. Crystalline cadmium sulfide (CdS) is now regarded as one of the most attractive visible light-driven photocatalysts due to its relatively narrow bandgap (2.42 eV), fitting well within the solar spectrum [3,4]. However, the direct application of CdS particles within the industrial sector is limited by the high cost of the concomitant filtration facilities for CdS recovery [5]. For this reason, a variety of CdS nanostructures such as nanocrystals, nanowires and nanoribbons have been explored with arrested precipitation approach, templating against inorganic (such as porous anodized aluminum oxide (AAO), carbon nanotube, SiO_2 and charcoal) [6–8] or organic (such as liquid crystals, micelles and polymer) substrates [9,10]. Specifically, high-quality substrate-supported CdS nanoparticles have exhibited excellent properties for various applications due to high specific area and low dimensionality [11,12]. Recently organic–inorganic hybrids have emerged as a new type of composites with interesting mechanical, optical, electrical and thermal properties, rather different from those of the starting materials. The immobilization of CdS on petrochemicals-derived polymer substrates including PVP, poly(ethylene glycol) (PEG)–block–poly(ethylene imine) (PEI) and nafion membrane has been the focus of many efforts [13–15].

Recent developments for cleaner, sustainable chemistry are being driven by a shift from petrochemical-based feedstocks to environmentally friendly biomaterials [16,17]. Among them, bacterial cellulose (BC) produced by fermentation of *Acetobacter xylinum* is of great interest due to its unique specific structure [18,19] and properties such as good mechanic properties, good chemical stability, high purity, high crystallinity and good compatibility [20–22]. The ultra fine three-dimension networks endow BC with well-separated nano- and microfibrils (width < 100 nm), distinct tunnel and pore structure, which create extensive specific area. Hence, BC has found wide applications for both biomaterials and template or matrix for the synthesis of various inorganic nanostructures [23,24].

Recently, we reported the preparation of TiO_2/BC hybrid nanofibers as UV light-sensitive photocatalyst [25], Pd–Cu/BC nanofibers as catalyst for water denitrification [26], and Pt nanoparticle-embedded BC membrane for fuel cell application [27]. As an extension of our research efforts to develop BC-inorganic hybrid nanofibers based functional materials, we report herein our research work in the preparation of morphology-controlled CdS nanocrystals and the potentiality of CdS/BC hybrid nanofibers as high-efficiency photocatalyst. The hybrid nanofibers were prepared by hydrothermal method. The resulting CdS/BCF

* Corresponding author. Fax: +86 25 84315079.
** Corresponding author. Fax: +86 25 84317311.
E-mail addresses: dongpingsun@163.com (D. Sun), whtang@mail.njust.edu.cn (W. Tang).

0304-3894/$ – see front matter © 2011 Elsevier B.V. All rights reserved.
doi:10.1016/j.jhazmat.2011.02.048

hybrid nanofibers were characterized by X-ray diffraction (XRD), transmission electron microscopy (TEM), and X-ray photoelectron spectroscopy (XPS) techniques. The excellent photocatalytic activity of the novel CdS/BCF hybrid nanofibers under visible light was also demonstrated.

2. Experimental

2.1. Preparation of hybrid CdS/bacterial cellulose fiber

The pristine BC substrate was synthesized and purified as reported [25]. The BC fibers were rinsed with deionized water (pH 7) and stored at 4 °C for use. The preparation of CdS/BC hybrid nanofiber involves a hydrothermal reaction as a key step. The as prepared BC fibers were first immersed into a mixture solution of ethanol and water (50:50, v/v). A following solvent exchange process was performed by stepwise increasing the ethanol content up to 99% to remove disordered water. The ethanol-saturated BC fibers were centrifuged before adding into 200 mL hydrothermal reaction mixture solution of $CdCl_2$, thiourea in ethanol. The reaction was carried out at 30 °C for 2 h with mechanical stirring (ca. 200 rpm). Subsequently, the mixture solution was transferred into a teflon tube fit within a stainless steel autoclave. The autoclave was then sealed and heated for either 3 h, 5 h or 7 h in a preheated oven (180 °C). The reaction mixture was centrifuged to obtain the titled CdS/BC hybrid nanofibers. The fibers were further washed with deionized water and ethanol three times separately, and finally dried overnight *in vaccuo* at 60 °C. For crystallization comparison, pristine CdS particles were prepared using the similar 5 h-hydrothermal process in the absence of BC fiber.

2.2. Characterization of hybrid fiber

The morphology of pristine BC, CdS/BC hybrid nanofibers and pristine CdS particles was investigated by means of TEM (JEM-2100). The crystallinity and the phase composition of samples were characterized by XRD (Bruker D8 ADVANCE). UV–visible spectra were recorded on a Cary 5000 spectrophotometer equipped with an integrated sphere accessory for diffusive reflectance spectra. X-ray photoelectron spectroscopy (XPS) measurements were performed on a PHI-5300 X-ray photoelectron spectrometer with an Mg K_α excitation source (1253.6 eV). Thermogravimetric analyses (TGA) were performed on a Boyuan DTU-2C thermogravimetric analyzer from 30 to 600 °C at a heating rate of 10 °C min^{-1} in air flow.

2.3. Photocatalytic experiment

Methyl orange (MO) is commonly considered as a representative organic dye in textile effluents, which can easily be monitored by optical absorption spectroscopy. Herein, MO was applied as model contaminant in the photocatalytic decomposition to investigate the photocatalytic activity of the CdS/BC hybrid nanofibers. A set of photocatalytic degradation experiments were performed with the following procedure: suspensions of the hybrid nanofibers (200 mg) in MO aqueous solution (20 ppm) were placed in a quartz reactor (200 mL), which was equipped with a 300 W xenon lamp light source with the cutoff wavelength $\lambda < 420$ nm. Prior to the photoreaction, the solution was magnetically stirred in the dark for 1 h to reach adsorption/desorption equilibrium; then the stirring reaction solution was irradiated by the vertically incident visible light. During the photoreaction, samples were taken at every 10-min interval and centrifuged to obtain clear solutions for photo-optical analysis.

3. Results and discussion

3.1. Morphology of CdS/BCF hybrid nanofibers

The TEM images of bare BC nanofibers and the CdS/BCF hybrid nanofibers are presented in Fig. 1. The TEM image of Fig. 1a shows a sideview of the BC nanofibers biosynthesized by *Acetobacter xylinum* NUST5.2, with an average diameter of about 30 nm and a length ranging from micrometers up to dozens of micrometers. TEM images of the CdS/BCF hybrid nanofibers obtained by hydrothermal reaction for 3 h, 5 h and 7 h are shown in Fig. 1b–d, respectively. As shown in Fig. 1b, the deposited CdS nanocrystals were well-dispersed on BC surface with a 10–20 nm diameter. The CdS obtained after 5 h hydrothermal reaction exhibited larger particle size (ca. 30–50 nm in diameter). For prolonged reaction duration (7 h), the prepared CdS nanoparticles achieved significantly increased dimension (diameters ranging from 150 to 200 nm) and obvious aggregation of the nanoparticles were clearly observed (Fig. 1d). Fig. 1e shows the TEM images of pristine CdS particles formed without BC substrate, with the size varying in the range of 0.5–1 μm. These cubic CdS particles tend to aggregate into small clusters. It is evident that BC fibers can provide confined template during CdS growth.

It is worthy mentioning that the crystal growth sites along BCF are identical in Fig. 1b–d due to the same reaction system employed. Scheme 1 illustrates the entire procedure of the fabrication of CdS/BCF. At the beginning, when BCF was added into the $CdCl_2$ ethanol solution, the Cd^{2+} coordinate with two adjacent C2 and C3-hydroxyl groups in the same glucose units along the BC backbone [28]. Subsequently, when thiourea was added into the colloidal mixture, the Cd^{2+} was chelated with thiourea to form colorless quadridentate chelate. Finally, upon heating, thiosemicarbazide is attacked by the strong nucleophilic O atoms of H_2O molecules leading to the weakening of the C=S double bonds. Heated at elevated temperature, the C=S bond will be broken, and the S^{2-} anion will slowly generate, which then reacts with Cd^{2+} to form CdS particles [28,29]. The as-prepared CdS nanoparticles were stabilized on the BCF surface via coordination effect between CdS and hydroxyl groups of BCF, as shown in Scheme 1. This stability mechanism is similar to that of CdS nanoparticles capped by chitosan or cellulose [28,29]. This growth mechanism is in good agreement with the above-presented TEM photographs and the following XRD studies.

The crystallographic behavior of the deposited CdS nanoparticles was further investigated by X-ray diffraction (XRD). From the XRD spectra shown in Fig. 2, broad peaks are observed at 2θ values of 14.5°, 16.6°, and 22.5°, which are characteristic peaks for BC fibers and can be assigned to the crystallographic plane of (1 0 0), (1 $\bar{1}$ 0) and (2 0 0) reflection of BC, respectively [30,31]. Apart from the diffraction peaks of BC, there are several distinct peaks for the CdS/BC hybrid nanofibers. All of the rest diffraction peaks match well with those of the perfect hexagonal wurtzite-structured CdS. The hexagonal wurtzite-structured CdS crystals present lattice parameters of $a = 4.14$ Å and $c = 6.72$ Å, in a good agreement with the literature values (JCPDS Card, No. 41-1049) [32,33]. No extra peaks are detected in these patterns, indicating clean CdS/BC composites achieved without any impurities. It should be noted that the diffraction peaks increase in intensity with narrower breadth when deposited CdS nanoparticles with longer hydrothermal reaction. The broader diffraction peaks for the CdS/BC hybrid fiber also lead to smaller average particle size as calculated by the Scherrer equation. The calculation results, which estimated the average size to be 26.4 nm, 58.7 nm and 239.1 nm for CdS/BC hybrid fiber of 3 h, 5 h and 7 h, are in good agreement with TEM measurements. Compared with the diffraction pattern of sample (CdS/BCF), an extra diffraction peak at 30.6° was observed for pristine CdS particles. As

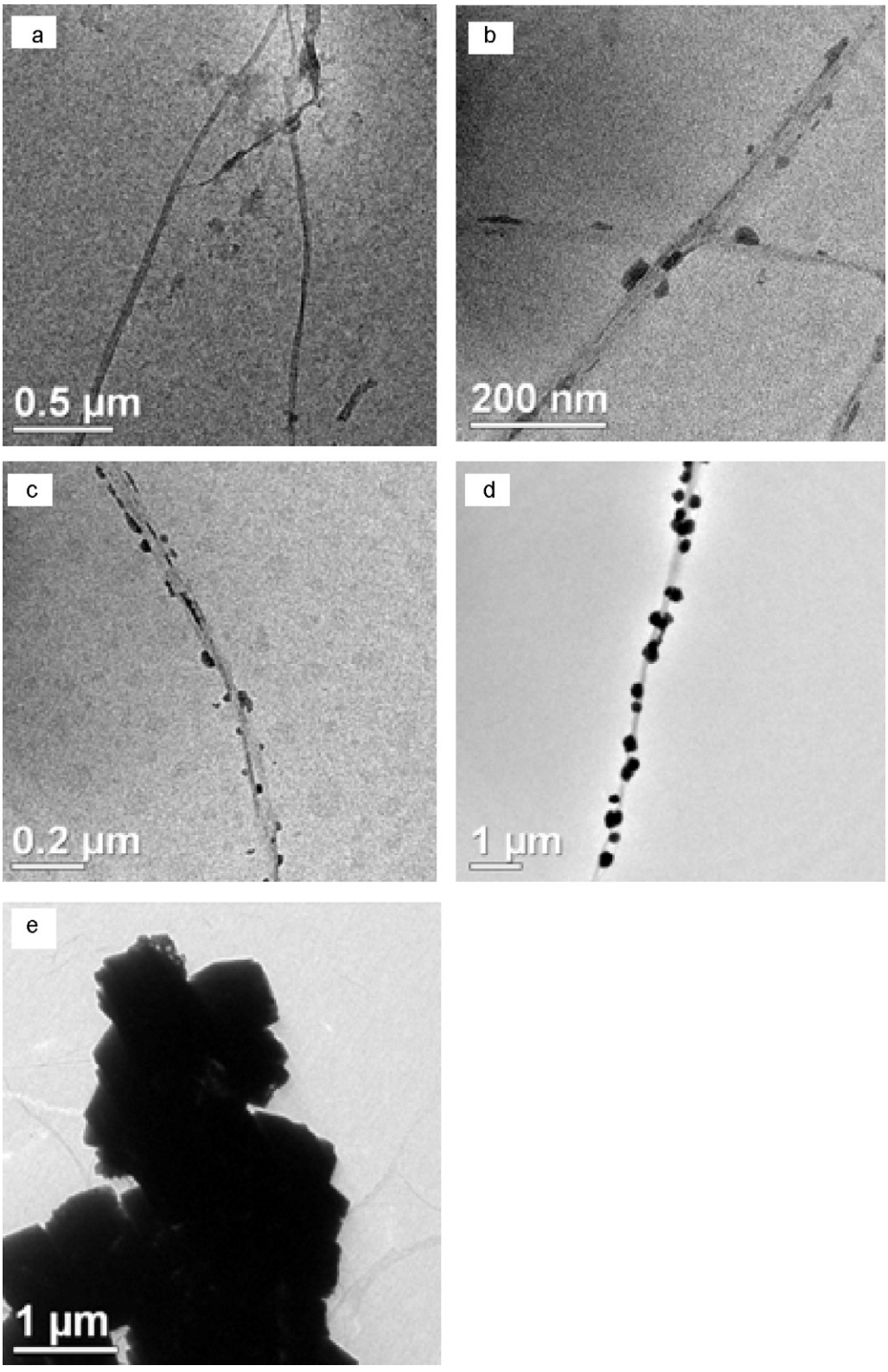

Fig. 1. TEM images of pristine BC nanofibers (a) and the CdS/BCF hybrid nanofibers prepared with hydrothermal reaction for 3 h (b), 5 h (c), and 7 h (d). (e) Reference CdS particles prepared with hydrothermal reaction for 5 h without BC substrate.

is known, the hexagonal structure CdS has no characteristic diffraction peak at 30.6°. According to JCPDS No: 10-0454, cubic structure of CdS typically has a characteristic peak at 30.6° corresponding to the (2 0 0) plane. It clearly indicates that two crystalline phases, cubic and hexagonal phases, coexist in pristine CdS particles. It is interesting that the hexagonal phase for CdS was obtained at such a low temperature in our hydrothermal route. According to Sun and Li [34], the temperature at which CdS nanocrystal changes from the amorphous phase to the hexagonal phase at 180 °C and a nearly complete hexagonal phase was at 240 °C in their hydrothermal method. It is evident that BC fibers can induce the growth of hexagonal phase CdS nanocrystals.

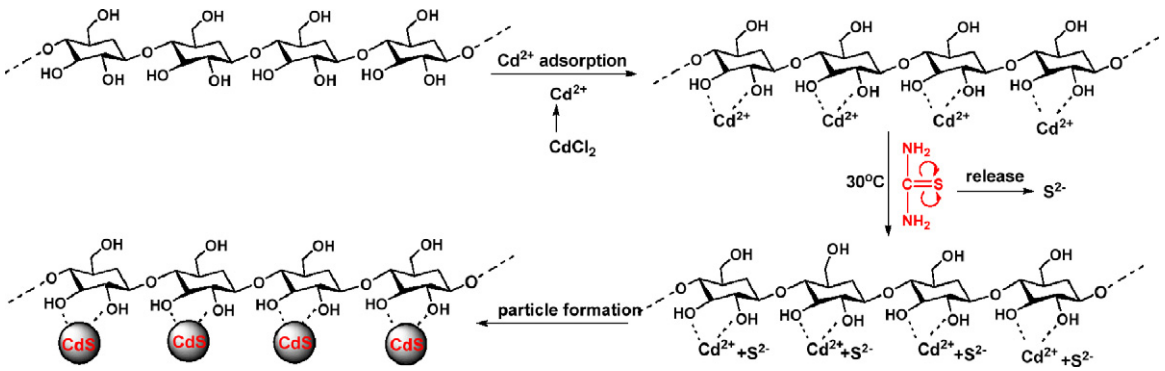

Scheme 1. Schematic illustration of the preparation of CdS/BC hybrid nanofibers.

Further evidence of the high crystal quality was obtained using X-ray photoelectron spectroscopy (XPS). From Fig. 3a–b, the binding energies of S $2p_{3/2}$, Cd $3d_{3/2}$ and Cd $3d_{5/2}$ are identified at 161.2 eV, 411.9 eV and 404.7 eV, respectively, which is consistent with the reported values in the literature [35,36]. These results further confirmed the nanocrystals are pure CdS, as proven in the XRD spectra. By estimation of the peak areas of the selected XPS peaks, the Cd-to-S atomic ratio at the surface was determined to be 1.09, which was close to the theoretical values, indicating that almost all precursor Cd^{2+} ions have transformed into CdS nanoparticles.

3.2. Photo-optical measurements

The as-prepared hybrid nanofibers present the typical band-to-band absorption in the visible spectral region because of the incorporated CdS nanoparticles, whereas the empty BCF matrix does not show any prominent optical absorption in the similar spectral region (Fig. 4a). The color of the empty BCF matrix is milky. It is noteworthy that the CdS/BC composites exhibit red-shifted absorption spectra with prolonged reaction time. When heating time increased from 3 h to 5 h, the corresponding composites show a maximum absorption peak at 475 nm and 483 nm, respectively. Further prolonging the reaction time to 7 h, the composites display a much red-shifted maximum absorption peak (498 nm), accompanying a significant increase in the absorbance intensity. The red-shifted and intensified absorption spectra at longer reaction time could result from the increased mean particle size of CdS crystals due to further crystalline growth during the afterward reaction time. These results are coincident with those obtained from TEM photographs and XRD patterns. As observed by naked eyes, the ethanol solution of dispersed composites changed in color from lemon to bright yellow, and further to deep yellow as the reaction time prolongs from 3 h to 5 h, and further to 7 h (Fig. 4b). Compared with CdS bulk material, which shows maximum absorption peak around 520 nm, all of the CdS/BCF hybrid nanofibers

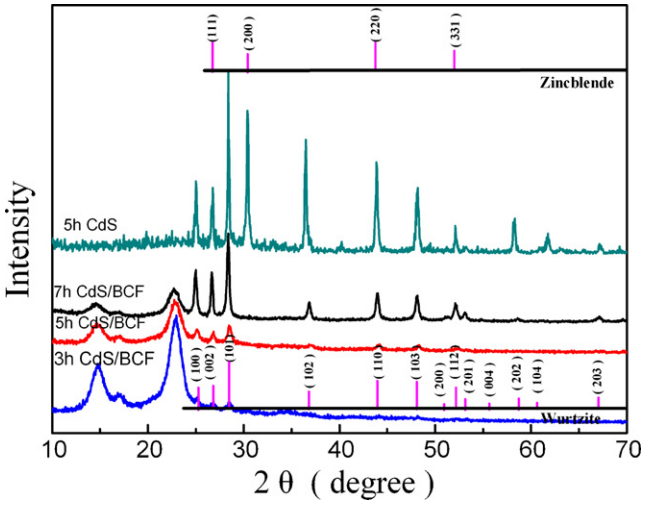

Fig. 2. X-ray diffraction (XRD) patterns of CdS/BCF hybrid nanofibers prepared at 180 °C for 3 h, 5 h, and 7 h, respectively. Reference CdS particles prepared with hydrothermal reaction for 5 h without BC substrate assigned as 5 h CdS.

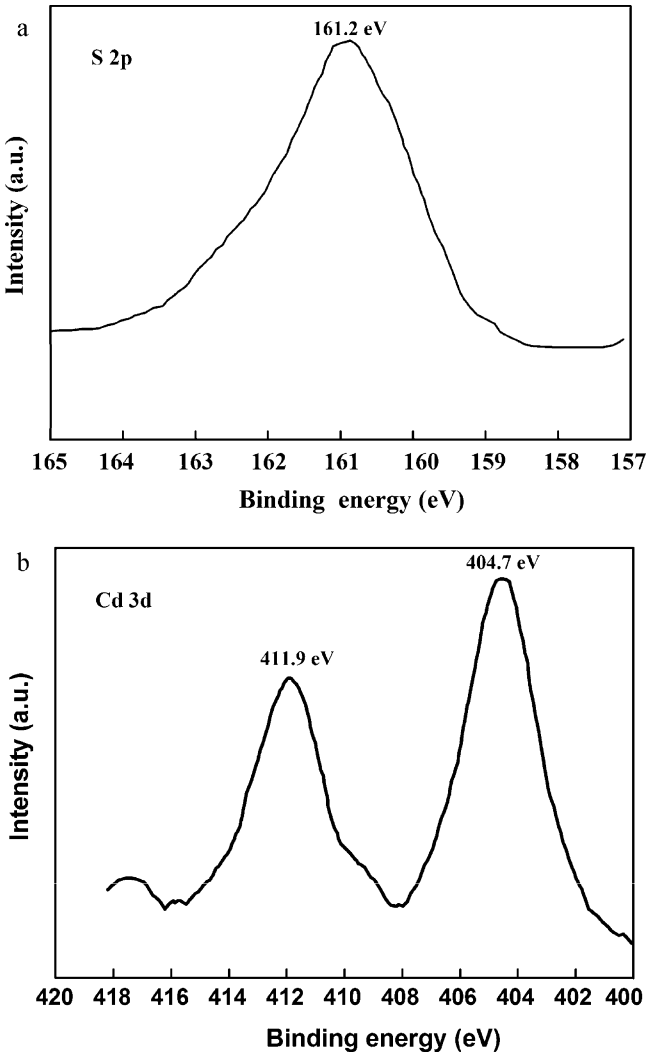

Fig. 3. XPS analysis of the CdS/BCF hybrid nanofibers: (a) S-2p binding energy spectrum and (b) Cd-3d binding energy spectrum.

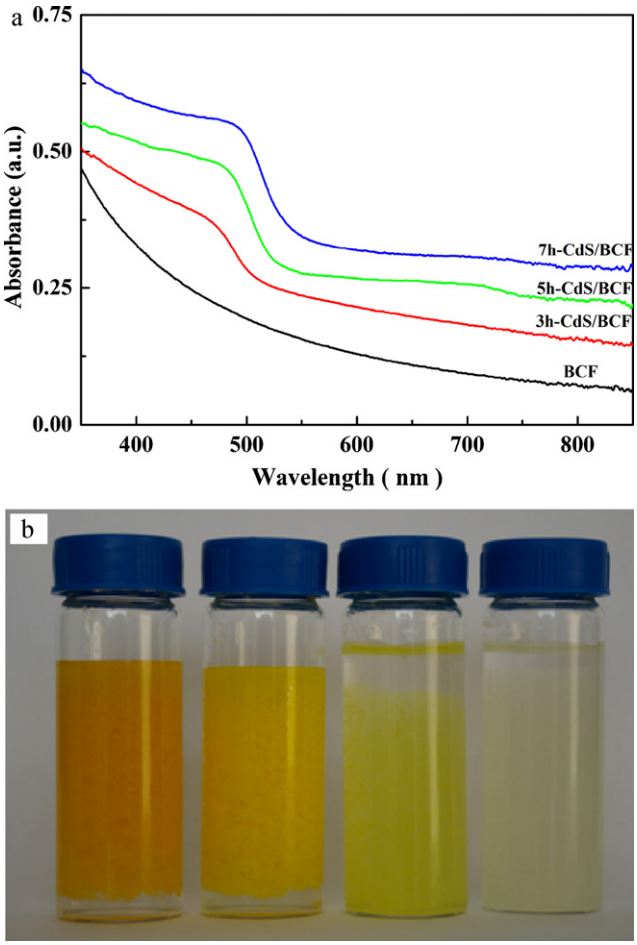

Fig. 4. (a) UV–vis absorption spectra of BC nanofibers and CdS/BCF hybrid nanofibers prepared at 180 °C for 3 h, 5 h, and 7 h. (b) Photograph image of the nanofibers and CdS/BCF hybrid nanofibers prepared at 180 °C for 3 h, 5 h, and 7 h.

have shown considerable blue-shifted absorption spectra due to quantum confinement [37]. Similar behavior was observed in the synthesis of CdS nanopaticles by using double-hydrophilic block copolymers of solvating PEG block and binding PEI block [14].

The thermal stability of the pristine BC fibers and CdS/BC hybrid nanofibers (hydrothermal reaction 5 h) was evaluated by thermogravimetric analysis (TGA) in air flow (Fig. 5). It is apparent that CdS/BC hybrid nanofibers exhibited better thermal stabilities than BC fibers, as weight loss less than 5% on heating to 340 °C for the former and 270 °C for the latter. Upon continuous heating up to 600 °C, pure BC degrades completely, leaving only minute amounts, while 40% of the sample still remains in CdS/BCF. Black ashes were obtained after the measurement of CdS/BCF.

The photocatalytic activities of the CdS/BC hybrid nanofibers were evaluated by photocatalytic degradation of MO under visible light irradiation. As a control, the activity of commercial photocatalyst P25 and pristine CdS particles were also tested under same conditions. Results of the photocatalytic evaluation are shown in Fig. 6a. Obviously, the removal rate of photocatalytic degradation of MO with the CdS/BCF hybrid nanofibers (5 h hydrothermal reaction) is much higher than that of commercial photocatalyst P25 and pristine CdS particles. In order to get the accurate kinetic data, kinetic experiments were carried out after 60 min dark reaction to assure the adsorption equilibrium was reached. It is well-known that photocatalytic oxidation of organic pollutants obeys Langmuir–Hinshelwood kinetics [38]. This kind of pseudo-first-

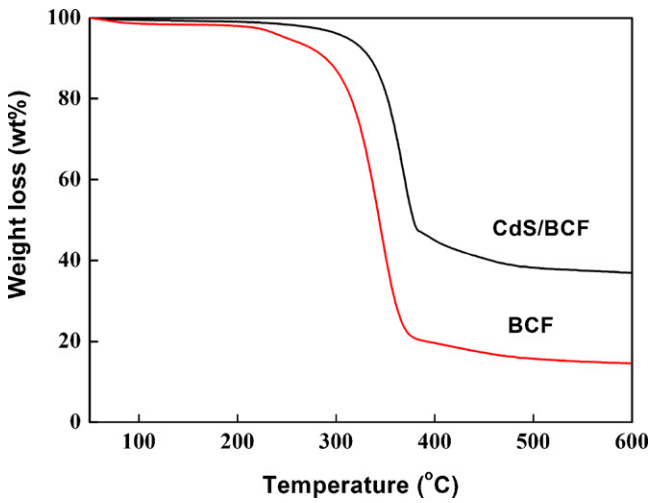

Fig. 5. TGA traces of BC nanofibers and CdS/BCF hybrid nanofibers (hydrothermal reaction 5 h) recorded at a heating rate of 10 °C min^{-1} under air flow.

order kinetics can be represented as follows:

$$r = -\frac{dC}{dt} = -\frac{k_r KC}{1 + KC} \quad (1)$$

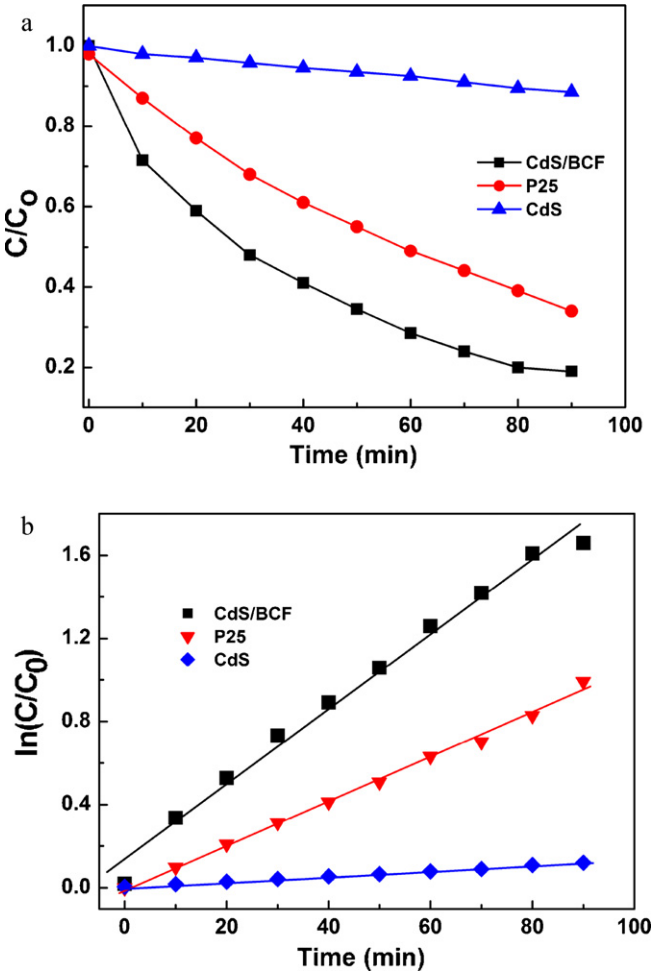

Fig. 6. Effect of illumination time on the degradation of MO in the presence of CdS/BCF under visible light irradiation (top panel) and plot of ln(C/C_0) versus irradiation time (bottom panel).

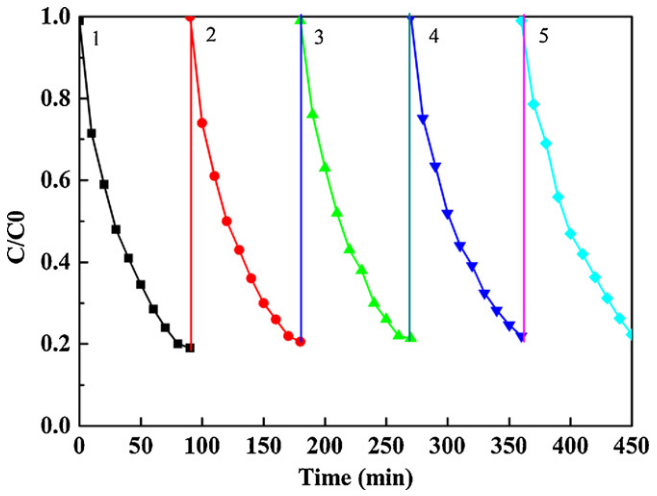

Fig. 7. The decrease of MO concentration with visible light irradiation by recycling use of CdS/BCF.

where r is the rate of dye mineralization, k' is the rate constant, C is the dye concentration, and K is the adsorption coefficient. By integration, Eq. (1) can be arranged into the following:

$$\ln\left(\frac{C}{C_0}\right) = -kt \tag{2}$$

where C_0 is the initial concentration of the MO solution and k is a rate constant.

According to Eq. (2), rate constant k can be given by the slope of fitting curves, when plotting $\ln(C/C_0)$ against. The degradation data of MO in the presence of CdS/BCF hybrid nanofibers, commercial photocatalyst P25 and pristine CdS particles are plotted in Fig. 6b, shown with the linear fitting curves. The reaction rate constants for CdS/BCF hybrid nanofibers, commercial photocatalyst P25 and CdS are 0.012 min^{-1}, 0.0104 min^{-1}, and 0.00013 min^{-1}, respectively. The results illustrate that the CdS/BCF to be a better photocatalyst than P25 in the visible light irradiation.

From a practical viewpoint, it is utmost necessary to evaluate the stability and reusability of CdS/BCF. The photocatalytic experiments were repeated 5 times with the same catalyst at 20 mg/L MO concentration in the presence of 200 mg/L catalyst. After each experiment, the catalyst was taken out by the filtration, washed and recycled. The results showed that the catalytic activity of the catalyst had a slight decrease after 5 cycles and the results were shown in Fig. 7. The degradation rates for 5-cycle reuses were 82%, 80.4%, 78.6%, 78%, and 77.3%, respectively, after 90-min irradiation. The photocatalytic reactivity of the present photocatalyst is just slightly reduced in stirred aqueous solution, indicating that cycling usage of the photocatalyst is possible and its stability in treating polluted water is satisfactory.

4. Conclusions

In summary, a facile approach to fabricate CdS/BCF hybrid nanofibers with high photocatalytic activity has been proposed. Nanocrystals of CdS with well-defined hexagonal wurtzite structure were obtained with size controllable by reaction time. The as-used hydrothermal method is effective to achieve CdS-embedded BC hybrid composites. The results of TEM, XRD and XPS analysis confirmed the growth process of CdS nanoparticles. Red-shifted absorption spectra on the hybrid nanofibers synthesized at increased reaction time indicate the crystalline growth of CdS nanoparticle at the original crystalline nuclei. The photocatalysis ability of the newly developed CdS/BCF hybrid nanofibers was evaluated by MO degradation. The results indicate that the robust BCF-supported CdS nanoparticles are effective in photocatalysis of organic dyes like MO. In addition, shape and size controlled CdS cemented on renewable BC nanofibers offer the potentialities as recyclable photocatalyst in the area of the catalytic processes.

Acknowledgments

The authors acknowledged the financial support from the National Natural Science Foundation of China (Nos. 10776014 and 21074055) and NUST Research Funding (No. 2010ZDJH04).

References

[1] J.A. Lee, K.C. Krogman, M. Ma, R.M. Hill, P.T. Hammond, G.C. Rutledge, Highly reactive multilayer-assembled TiO_2 coating on electrospun polymer nanofibers, Adv. Mater. 20 (2008) 1252–1256.
[2] C. Burda, Y. Lou, X. Chen, A.C.S. Samia, J. Stout, J.L. Gole, Enhanced nitrogen doping in TiO_2 nanoparticles, Nano Lett. 3 (2003) 1049–1051.
[3] G. Dukovic, M.G. Merkle, J.H. Nelson, S.M. Hughes, A.P. Alivisatos, Photodeposition of Pt on colloidal CdS and CdSe/CdS semiconductor nanostructures, Adv. Mater. 20 (2008) 4306–4431.
[4] J. Cao, J.Z. Sun, J. Hong, H.Y. Li, H.Z. Chen, M. Wang, Carbon nanotube/CdS core–shell nanowires prepared by a simple room-temperature chemical reduction method, Adv. Mater. 16 (2004) 84–87.
[5] S. Suarez, J. Coronado, R. Portela, J.C. Martin, M. Yates, P. Avila, B. Sanchez, On the preparation of TiO_2–Sepiolite hybrid materials for the photocatalytic degradation of TCE: influence of TiO_2 distribution in the mineralization, Environ. Sci. Technol. 42 (2008) 5892–6589.
[6] B. Cao, Y. Jiang, C. Wang, W.H. Wang, L.Z. Wang, M. Niu, W.J. Zhang, Y.Q. Li, S.T. Lee, Synthesis and lasing properties of highly ordered CdS nanowire arrays, Adv. Funct. Mater. 17 (2007) 1501–1506.
[7] J.H. Shi, Y.J. Qin, W. Wu, X.L. Li, Z.X. Guo, D.B. Zhu, In situ synthesis of CdS nanoparticles on multi-walled carbon nanotubes, Carbon 42 (2004) 455–458.
[8] H.J. Liang, T.E. Angelini, P.V. Braun, G.C.L. Wong, Roles of anionic and cationic template components in biomineralization of CdS nanorods using self-assembled DNA–membrane complexes, J. Am. Chem. Soc. 126 (2004) 14157–14165.
[9] Y. Zhou, Q. Ji, M. Masuda, S. Kamiya, T. Shimizu, Helical arrays of CdS nanoparticles tracing on a functionalized chiral template of glycolipid nanotubes, Chem. Mater. 18 (2006) 403–406.
[10] T. Hirai, M. Ota, Immobilization of CdS nanoparticles from reverse micellar system onto mesoporous organosilicates and their photocatalytic properties, Mater. Res. Bull. 41 (2006) 19–28.
[11] C.S. Yang, D.D. Awschalom, G.D. Stucky, Kinetic-dependent crystal growth of size-tunable CdS nanoparticles, Chem. Mater. 13 (2001) 594–598.
[12] P. Zhang, L. Gao, Synthesis and characterization of CdS nanorods via hydrothermal microemulsion, Langmuir 19 (2003) 208–210.
[13] J.H. Zeng, Y. Zhu, Y.F. Liu, J. Yang, Y.T. Qian, H.G. Zheng, Morphology development of CdS/PVAc composite from spheres to rods, Mater. Sci. Eng. B 94 (2002) 131–135.
[14] L.M. Qi, H. Colfen, M. Antonietti, Synthesis and characterization of CdS nanoparticles stabilized by double-hydrophilic block copolymers, Nano Lett. 1 (2001) 61–65.
[15] S.M. Wang, P. Liu, X.X. Wang, X.Z. Fu, Homogeneously distributed CdS nanoparticles in Nafion membranes: preparation, characterization, and photocatalytic properties, Langmuir 21 (2005) 11969–11973.
[16] M. Chtchigrovsky, A. Primo, P. Gonzalez, K. Molvinger, M. Robitzer, F. Quignard, F. Taran, Functionalized chitosan as a green, recyclable, biopolymer-supported catalyst for the [3+2] Huisgen cycloaddition, Angew. Chem. Int. Ed. 48 (2009) 5916–5920.
[17] C.E. Song, S.G. Lee, Supported chiral catalysts on inorganic materials, Chem. Rev. 102 (2002) 3495–3524.
[18] J. Juntaro, M. Pommet, G. Kalinka, A. Mantalaris, M.S.P. Shaffer, A. Bismarck, Creating hierarchical structures in renewable composites by attaching bacterial cellulose onto sisal fibers, Adv. Mater. 20 (2008) 3122–3126.
[19] M. Nogi, H. Yano, Transparent nanocomposites based on cellulose produced by bacteria offer potential innovation in the electronics device industry, Adv. Mater. 20 (2008) 1849–1852.
[20] H. Yano, J. Sugiyama, A.N. Nakagaito, M. Nogi, T. Matsuura, M. Hikita, K. Handa, Optically transparent composites reinforced with networks of bacterial nanofibers, Adv. Mater. 17 (2005) 153–155.
[21] G. Guhados, W.K. Wan, J.L. Hutter, Measurement of the elastic modulus of single bacterial cellulose fibers using atomic force microscopy, Langmuir 21 (2005) 6642–6646.
[22] D. Klemm, B. Heublein, H.P. Fink, A. Bohn, Cellulose: fascinating biopolymer and sustainable raw material, Angew. Chem. Int. Ed. 44 (2005) 3358–3393.
[23] W. Czaja, S.A. Krystynowicz, R. Brown, M. Bielecki, Microbial cellulose-the natural power to heal wounds, Biomaterials 27 (2006) 145–151.
[24] Y.Z. Wan, L. Hong, S.R. Jia, Y. Huang, Y. Zhu, Y.L. Wang, H.J. Jiang, Synthesis and characterization of hydroxyapatite–bacterial cellulose nanocomposites, Compos. Sci. Technol. 66 (2006) 1825–1832.

[25] D.P. Sun, J.Z. Yang, X. Wan, Bacterial cellulose/TiO_2 hybrid nanofibers prepared by the surface hydrolysis method with molecular precision, Nanoscale 2 (2010) 287–292.
[26] D.P. Sun, J.Z. Yang, L. Jun, J.W. Yu, X.F. Xu, X.J. Yang, Novel Pd–Cu/bacterial cellulose nanofibers: preparation and excellent performance in catalytic denitrification, Appl. Surf. Sci. 256 (2010) 2241–2244.
[27] J.Z. Yang, D.P. Sun, J. Li, X.J. Yang, J.W. Yu, Q.L. Hao, In situ deposition of platinum nanoparticles on bacterial cellulose membranes and evaluation of PEM fuel cell performance, Electrochim. Acta 54 (2009) 6300–6305.
[28] R. Jiang, H. Zhu, X. Li, L. Xiao, Visible light photocatalytic decolourization of C. I. Acid Red 66 by chitosan capped CdS composite nanoparticles, Chem. Eng. J. 152 (2009) 537–542.
[29] A. Kumar, V. Kumar, Self-assemblies from RNA-templated colloidal CdS nanostructures, J. Phys. Chem. C 112 (2008) 3633.
[30] C. Tokoh, K. Takabe, M. Fujita, H. Saiki, Cellulose synthesized by *Acetobacter xylinum* in the presence of acetyl glucomannan, Cellulose 5 (1998) 249–261.
[31] W. Czaja, D. Romanovicz, R.M. Brown, Structural investigations of microbial cellulose produced in stationary and agitated culture, Cellulose 11 (2004) 403–411.
[32] J. Puthussery, A. Lan, T.H. Kosel, M. Kuno, Band-filling of solution-synthesized CdS nanowires, ACS Nano 2 (2008) 357–367.
[33] P. Zhang, L. Gao, Synthesis and controlling the morphology of CdS nanocrystals via hydrothermal microemulsions, J. Colloid Interface Sci. 272 (2004) 99–103.
[34] S.Q. Sun, T. Li, Synthesis and characterization of CdS nanoparticles and nanorods via solvo-hydrothermal route, Cryst. Growth Des. 7 (2007) 2367–2371.
[35] S.L. Xiong, X.G. Zhang, Y.T. Qian, CdS with various novel hierarchical nanostructures by nanobelts/nanowires self-assembly: controllable preparation and their optical properties, Cryst. Growth Des. 9 (2009) 5259–5265.
[36] T.Y. Zhai, X.S. Fang, Y. Bando, Q. Liao, X.J. Xu, H.B. Zeng, Y. Ma, J.N. Yao, D. Golberg, Morphology-dependent stimulated emission and field emission of ordered CdS nanostructure arrays, ACS Nano 3 (2009) 949–959.
[37] W.S. Chae, S.W. Lee, M.J. An, K.H. Choi, S.W. Moon, W.C. Zin, J.S. Jung, Y.R. Kim, Nanostructures and optical properties of mesoporous composite nanofibers containing CdS quantum dots, Chem. Mater. 17 (2005) 5651–5657.
[38] R.K. Wahi, W.W. Yu, Y.P. Liu, M.L. Mejia, J.C. Falkner, W. Nolte, V.L. Colvin, Photodegradation of Congo Red catalyzed by nanosized TiO_2, J. Mol. Catal. A: Chem. 242 (2005) 48–56.